



## Research article

# Optimization and green metrics analysis of the liquid-phase synthesis of *sec*-butyl levulinate by esterification of levulinic acid with 1-butene over ion-exchange resins

Jordi H. Badia <sup>a</sup>, Eliana Ramírez <sup>a,\*</sup>, Rodrigo Soto <sup>a,b</sup>, Roger Bringué <sup>a</sup>, Javier Tejero <sup>a</sup>, Fidel Cunill <sup>a</sup>

<sup>a</sup> Chemical Engineering and Analytical Chemistry Department, University of Barcelona, Martí i Franquès 1-11, 08028 Barcelona, Spain

<sup>b</sup> Department of Chemical and Environmental Sciences, Synthesis and Solid State Pharmaceutical Centre (SSPC), University of Limerick, Limerick V94 T9PX, Ireland



## ARTICLE INFO

## Keywords:

Biomass  
Ion-exchange resins  
Olefin as an alternative esterifying agent  
Yield optimization  
Green metrics analysis  
Sec-butyl levulinates

## ABSTRACT

Liquid-phase esterification of levulinic acid (LA) with 1-butene (1B) over ion-exchange resins was studied following an experimental design approach aimed at identifying the optimal conditions to synthesize *sec*-butyl levulinate (SBL) through the proposed reaction pathway. Experiments were performed in a temperature range of 313–383 K with initial molar ratios of LA to 1B ( $R_{LA/1B}^0$ ) from 0.4 to 3. The optimal experimental conditions determined at 373 K and  $R_{LA/1B}^0 = 0.5$  render 1B and LA yields to SBL of 48.1% and 76.8%, respectively. Empirical equations relating conditions and yields were obtained, and response surface methodology analysis with subsequent multiobjective optimization allowed identification of optimal conditions to maximize simultaneously the yield of both reactants to SBL—that is high 1B initial concentration and temperature ranging 360–370 K. According to screening experiments, dense polymer network favors SBL formation. Amberlyst™15 was the most promising catalyst among the tested ones, since it yields the highest conversion with very low side reactions extension. A green metrics analysis was performed to ascertain the sustainability of the proposed chemical route and to compare it with previously reported studies for the SBL synthesis. Among the scenarios assessed, the proposed chemical pathway represents the greenest alternative.

## 1. Introduction

The ever-growing energy demand and the decay of fossil fuel resources over the last decades have led to the need for seeking alternatives to conventional fossil resources. The current energy paradigm claims for a transition to cleaner and more sustainable energy resources to meet the goals proposed in the Paris Agreement 2015, such as decreasing up to 2 °C the global Earth temperature as well as the reduction of greenhouse gas emissions [1]. Nowadays, measures are being implemented to palliate greenhouse gases emissions from combustion vehicles. In such scenario, one of the most promising alternatives in the short term relies on the use of biomass-derived fuels, which can help reducing non-renewable carbon emissions [2]. Both classical and biofuels produce CO<sub>2</sub> during combustion. However, the main advantage of using biofuels with respect to classical fuels is that they are considered carbon neutral because are produced from biomass, which is a renewable source of energy that indeed fixes CO<sub>2</sub> thereby contributing

to a more sustainable carbon net balance in the environment. Biofuels are chemical compounds derived from biomass that can feed combustion engines [3], and are currently classified into two levels: The first generation biofuels that are obtained from food crops (e.g. corn, sugar cane), and the second generation congeners that are linked to lignocellulosic-based materials from agricultural wastes and used cooking oils [4–6]. In principle, the rational choice leans towards the latter because they do not compete with the edible feedstock, yet they present significant difficulty for industrial scale-up. To overcome these limitations, efforts have been focused on conceiving new processes with alternative raw materials. For instance, other trends still under development have shown good results on a small scale using aquatic plants (third generation) and microorganisms (fourth generation) [7,8]

4-Oxopentanoic acid, also known as levulinic acid (LA), is an organic compound pinpointed as one of the top ten promising platform molecules by the US Energy Department in 2004 [9]. Among the broad number of chemical routes for its synthesis [10,11], the most widely

\* Corresponding author.

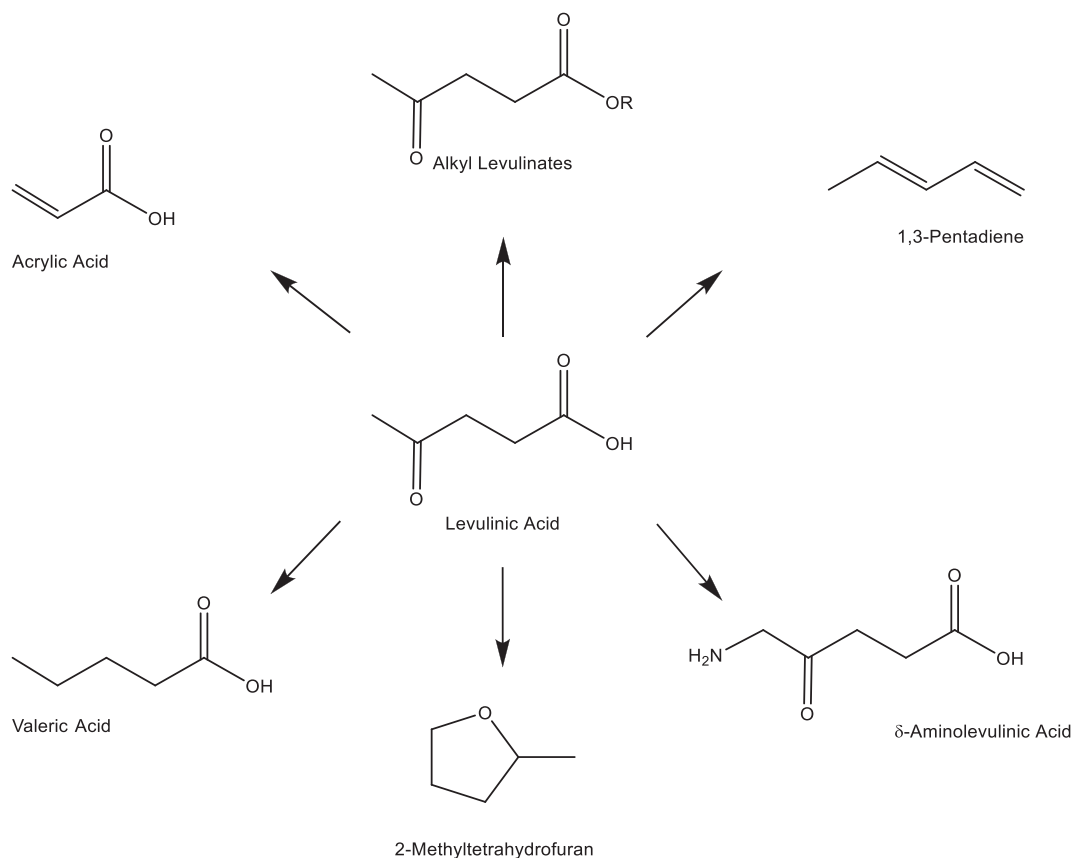
E-mail address: [eliana.ramirez-rangel@ub.edu](mailto:eliana.ramirez-rangel@ub.edu) (E. Ramírez).

<https://doi.org/10.1016/j.fuproc.2021.106893>

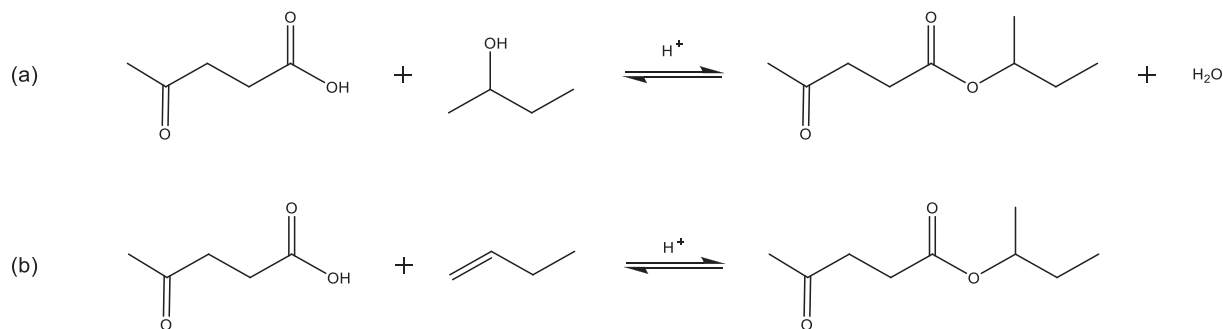
Received 26 April 2021; Accepted 10 May 2021

Available online 20 May 2021

0378-3820/© 2021 The Authors. Published by Elsevier B.V. This is an open access article under the CC BY license (<http://creativecommons.org/licenses/by/4.0/>).



**Scheme 1.** Some chemical derivatives obtained from levulinic acid. Adapted from [14].



**Scheme 2.** Esterification of levulinic acid over an acidic catalyst with (a) 2-butanol and (b) 1-butene.

used approach is called Biofine Process, employing lignocellulosic biomass as raw material [12]. Levulinic acid is a versatile molecule from which other chemicals with relevant applications can be obtained as shown in Scheme 1 [9,13]. For example, platform chemicals like acrylic acid, 1,3-pentadiene and valeric acid can be synthesized by catalytic reactions for the polymer and cosmetic industries, but also herbicides, pharmaceuticals, anti-freeze agents, or plasticizers, among others, can be obtained from LA [14]

Other outstanding derivatives of levulinic acid are alkyl levulinates, which have recently gained considerable attention as promising fuel additives for improving the efficiency of motor engines and reducing harmful emissions [15]. They can also enhance some physicochemical properties like viscosity, compressibility as well as pour and cloud points to perform the functions of lubricating, cleaning and stabilizing the fuel. Besides the application in the fuels field, alkyl levulinates have a broad range of uses in the flavoring and fragrance industries [16]. There exist different chemical routes to obtain these compounds; the most frequent

one is the esterification of levulinic acid with alcohol at moderate temperature in the presence of a homogeneous or heterogeneous catalyst (Scheme 2-a) [17]. Interestingly, there is also another promising route based on catalytic esterification of levulinic acid with an olefin such as 1-butene (Scheme 2-b) [18–21]. Some of the advantages of using olefins instead of alcohols encompass avoiding the formation of side-products and by-products as dialkyl ethers, water, and polymerization products, which can reduce the yield towards levulinate. Besides, in terms of reaction sustainability, olefinic esterification represents a greener synthesis than the alcohol-based route since both reagents are utterly incorporated into the product, showing a better esterification atom economy than when alcohols are used due to water formation.

An excellent review has recently emphasized the synthesis, potential applications, and fuel blending properties of levulinates [22]. Ethyl levulinate is the most widely studied levulinic ester, obtained either by homogeneous or heterogeneous catalysis [23]. Indeed, it has been taken into good consideration as a bio-based cold flow improver in biodiesel

fuels [24]. However, it presents some issues regarding phase instability below 0 °C in fuel blends. Some studies have revealed that butyl levulinates can be more suitable than the ethyl counterparts because of a lower solubility in water, a freezing point below −60 °C, and acceptable boiling and flash points for diesel engines [25,26]. On the other hand, reported values of blending octane number of methyl levulinate, ethyl levulinate, and iso- and *sec*-butyl levulinate are 106.5, 107.5, 102.5, and 102.5, respectively [27], which makes them potential candidate molecules for being included as high-octane gasoline components. Among these levulinates, methyl and ethyl levulinates, present higher miscibility in water and a tendency for separation from gasoline at low temperatures whereas both butyl levulinates can be regarded as more promising candidates because of their stronger similarities to other gasoline components.

Attempts on synthesizing levulinates from olefins date from 1970, but it is not until 2003 that butyl levulinate emerges as a potential candidate for fuel additives [19,28]. However, literature on *sec*-butyl levulinate synthesis is sparse (e.g., [29]). Relevant references on the subject would include recent works dealing with either homogeneous or heterogeneously-catalyzed processes and with the adequacy of using sulfonated polymeric materials as catalysts for the production of linear levulinates [18,30,31]. Despite better yields have been reported with homogeneous catalysis, the catalyst recovery entails a problem due to subsequent separation processes with detrimental operational costs. Therefore, there is a prevalence of using heterogeneous catalysts, which can be easily recovered and further reused. Acidic ion-exchange resins are excellent catalysts in many organic reactions such as dehydration of alcohols, etherification of olefins, and different condensation reactions [32–34].

One of the most common types of ion-exchange resins used in industry is composed of polystyrene-divinylbenzene (PS-DVB). The DVB content is related to the degree of crosslinking of polymer chains in a polystyrene matrix and it is an indicator of the structural stiffness. To provide a catalytic activity to the resins, chemical functionalization is required. Acidic ion-exchange resins are usually functionalized with sulfonic groups (−SO<sub>3</sub>H), which provide a strongly acidic behavior. A morphological classification arises into two groups of resins: gel-type (microporous) and macroreticular (macroporous) [33]. Gel-type resins are rigid beads that require a swelling medium (that is, a polar medium, such as water or alcohols) to expand the polymeric matrix and make the active sites accessible. Conversely, macroreticular resins present permanent porosity in the absence of an auxiliary medium.

The abovementioned scenario reflects manifold options for the production of SBL and highlights the necessity for a proper assessment of the different possibilities to pinpoint optimum conditions. Unfortunately, the comparison of the various proposed processes is often fuzzy due to the different reaction systems and/or experimental conditions. In particular, there is an obvious gap between laboratory-scale research and potential industrial application, since little effort has been devoted to adopting an engineering-type view of the reaction process. Therefore, key process variables such as operating temperature, reactants concentrations, best available catalysts, and catalyst-to-reagents ratio have never been investigated so far, despite being crucial to even consider potential industrial scale-up of the process. Furthermore, the environmental efficiency of the different processes needs also to be evaluated by means of a rational, biased-free methodology that allows proper comparison. In this regard, the use of the so-called green metrics analysis (GMA) offers a valuable tool for the evaluation of the “greenness” of each process that is useful for selecting the best possible synthetic route [35]. Not only it is of utility for comparing different synthesis plans, but also for optimizing existing processes in terms of materials, energy use, and waste reduction [36]. The success of the GMA relies on the translation of sustainable concepts into a mathematical language such that different approaches can be collated under a normalized procedure.

Therefore, the aim of the present work is to determine optimum reaction conditions for the esterification reaction of levulinic acid with 1-

butene, which can be done by means of a multivariable analysis coupled with a multiobjective optimization of reaction yields, to identify the best performing catalyst among a set of ion-exchange resins, which are well-known, environmentally friendly, cheap catalysts, and to evaluate the environmental sustainability of the proposed chemical route in comparison to other approaches reported in the literature through green metrics analysis performed at optimum conditions.

## 2. Materials and methods

### 2.1. Materials

The reactants used were levulinic acid (LA, 98% GC; Across Organics) and 1-butene (1B, >99.9% GC; Air Liquide). As chemical standards for chromatographic analyses 2-butanol (99% GC; Panreac) and butyl levulinate (98% GC; Sigma Aldrich) were used. Butyl levulinate was used instead of *sec*-butyl levulinate because it was not commercially available. From previous experience on the synthesis of butyl levulinate, it was found that these two ester molecules were almost identical in terms of chromatographic response [37]. Also, mass spectrum data obtained in the laboratory for both esters are provided in Fig. S1 and Fig. S2 of the Supporting Information.

On the other hand, the sulfonic styrene-divinylbenzene resins Amberlyst™ 15, Amberlyst™ 16, Amberlyst™ 39, Amberlyst™ 46, DOWEX™ 50Wx2–50 (A15, A16, A39, A46, and Dow2, respectively, The Dow Chemical Company, now DuPont), and Purolite® CT175 (CT175, Purolite) were used as catalysts. Their properties can be found in Table 3. These resins have been chosen because they can cover a wide variety of typical structural properties for this kind of catalyst.

### 2.2. Experimental setup and analytical system

Experimental runs were carried out in a batch reactor setup, which consisted of a 200 cm<sup>3</sup> stainless-steel jacketed batch reactor equipped with a six-blade magnetic stirrer (Autoclave Engineers, Pennsylvania, US). The reactor temperature was controlled within ±0.1 K by a 1,2-propanediol–water thermostatic mixture. GC–MS analyses of samples of the reaction medium allowed for quantifying the reactants and products concentrations during the runs. To this end, a sampling valve (Valco A2CI4WE.2, VICI AG International, Schenkon, Switzerland) was connected to the reactor vessel to inject 0.2 μL of pressurized liquid into an Agilent 6890 gas chromatograph coupled to a mass selective detector HP5973N (GC–MS). The GC was equipped with a capillary column (HP-PONA 19091S-001, J&W Scientific, Santa Clara, US; 100% dimethylpolysiloxane, 50 m × 0.20 mm × 0.50 μm). The electron source of the mass detector was set to 503 K and the quadrupole to 423 K. Helium, with a flow of 0.5 mL/min, was used as the carrier gas. GC oven temperature was set as follows: an initial hold of 6 min at 313 K, followed by a 35 K/min ramp to 473 K, and a final hold of 9 min. This analytical procedure allows identifying and quantifying all reactants, products, as well as main formed byproducts.

### 2.3. Experimental protocol

All experiments were carried out isothermally in the range 313–383 K and at 2.5 MPa, with a stirring speed of 750 rpm. The initial molar ratio between levulinic acid and 1-butene ( $R_{LA/1B}^{\circ}$ ) was varied between 0.4 and 3, while the total initial amount of reactants was maintained at about 2 mol. No solvents were used in any of the experiments. Before every experimental run, the catalyst was pretreated to reduce its moisture. Firstly, by drying at room temperature for 48 h, then in an atmospheric oven at 383 K for 2.5 h and, finally, in a vacuum oven at 0.001 MPa and 373 K for at least 12 h, until the experiment started. This procedure ensures a 3–5%wt. maximum final water content in the resin beads (as analyzed by Karl-Fischer titration in the laboratory).

In every experiment, a weighed amount of levulinic acid (ranging

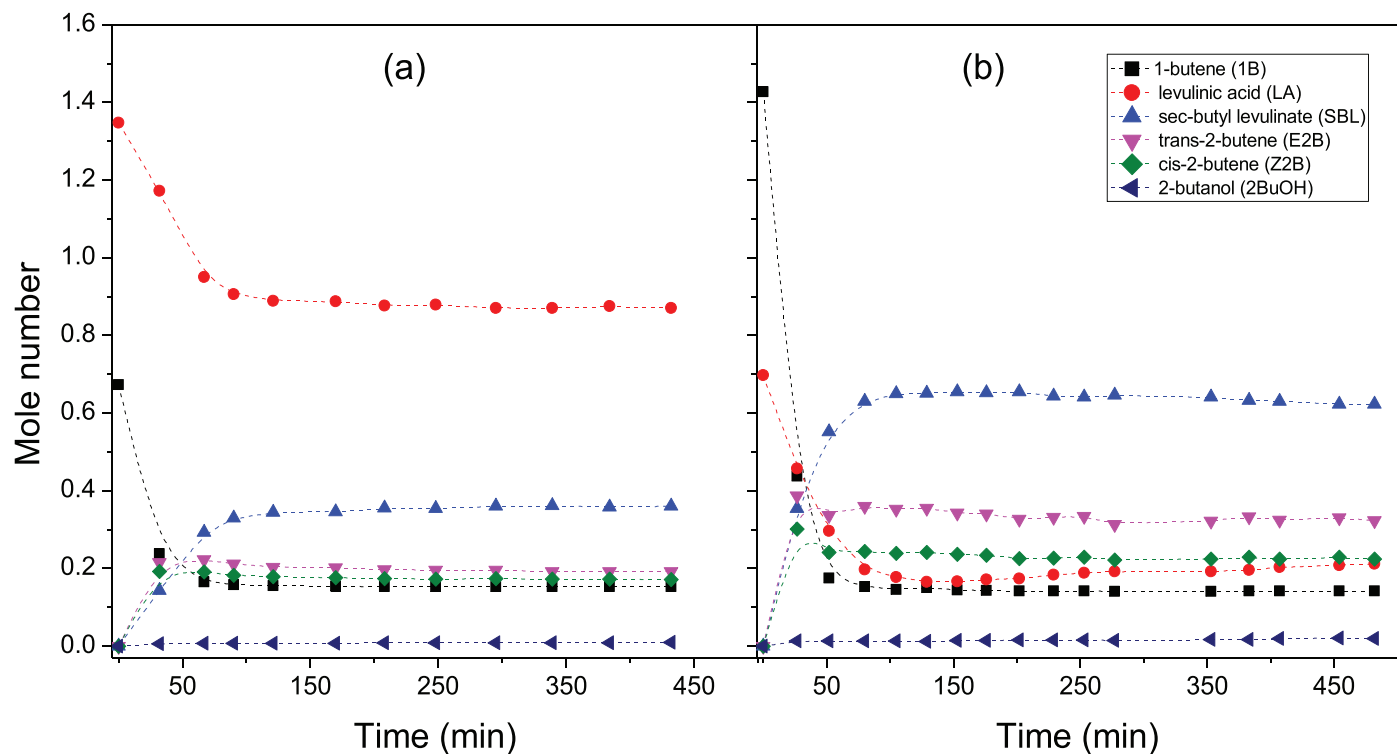


Fig. 1. Mole evolution of reaction species but oligomeric compounds for experiments at (a)  $R^o_{LA/1B} = 2.0$  (that is,  $x^o_{1B} = 0.33$ ) and (b)  $R^o_{LA/1B} = 0.50$  (that is,  $x^o_{1B} = 0.67$ ). Reaction conditions:  $T = 373$  K, stirring speed = 750 rpm, initial reactants load  $\approx 2$  mol, and catalyst load = 5 g of A15. Dashed lines are guides to the eye.

from about 68 to 180 g) was introduced into the reactor vessel and the heating and stirring were switched on. The corresponding amount of 1-butene was loaded into a pressurized burette by weight (29–86 g, approximately). Since the olefin is a gas at room conditions, it was liquefied by increasing the pressure in the burette to 0.5–1 MPa and finally introduced into the reactor by pressure difference, impelled by nitrogen. Once the reactants mixture reached the desired temperature, the catalyst was injected into the reactor by pressure difference with a catalyst injector attached to the reactor. The total reactor pressure at the beginning of each experiment was 2.5 MPa due to the described loading procedure, and it was kept constant throughout the whole experiment. Such pressure in the reactor allows to impel samples from the reactor to the GC and ensures that the reaction mixture remains in liquid phase. The injection of the catalyst marked the initial time of the experiment. From that moment onwards, samples were taken from the reactor every 30 min, approximately. Each run lasted for about 5–8 h. General calculations to characterize reaction medium (including conversion, selectivity, and yield) are indicated in Section B of the Supporting Information.

#### 2.4. Experimental design

A modified  $2^k$  factorial design was set to determine the range of operating conditions (that is, temperature,  $T$ , and molar fraction of 1-butene in the reactants mixture,  $x^o_{1B}$ ) to carry out the synthesis of sec-butyl levulinate using the proposed reaction pathway. The purpose of the present factorial design was to identify the optimal operating conditions using A15 as the catalyst, which are those maximizing the yield towards the main product. To provide an empirical relationship between operating conditions and yield towards the ester, a response surface methodology analysis was carried out through the stepwise multivariate regression procedure, using a second-order polynomial expression with interaction terms [38]:

$$y = \beta_0 + \sum_{m=1}^p \beta_m x_m + \sum_{m=1}^p \beta_{mm} x_m^2 + \sum_{m=1}^{p-1} \sum_{m<n}^p \beta_{mn} x_m x_n \quad (1)$$

where  $y$  is the response variable,  $x$  the independent variables, and  $\beta$  the equation coefficients. The proposed expression can describe the correlations between the significant predictor reaction variables ( $x_m$ — that is,  $T$  and  $x^o_{1B}$ ) and the predicted response ( $y$ — that is,  $Y_j^{SBL}$ ).

The experiments were carried out according to a two-variable, two-level, central composite design ( $2^2$  factorial design, with 4 additional points and 1 central point), which resulted in 9 experimental conditions, as depicted in Fig. S3 of the Supporting information (Section C).

#### 2.5. Green metrics analysis calculations

With regards to green metrics analysis calculations, among the wide number of metrics that can be evaluated [35,39–44], the most commonly used are defined as follows. The atom economy (AE) accounts for the number of reactants atoms incorporated into the chemical structure of the target reaction product. The reaction mass efficiency (RME) considers the involved masses of reactants and products. The stoichiometric factor (SF) quantifies the use of excess reactants. The mass recovery parameter (MRP) takes into account the use of additional materials, e.g. solvents, and its recovery in the reaction and post-reaction phases. These five parameters are frequently lumped together in a quadratic mean; the so-called Vector Magnitude Ratio (VMR). Also, the Environmental Factor ( $E_{\text{factor}}$ ) quantifies the amount of waste as the mass ratio of waste to the target product and may include the mass of auxiliary material ( $E_{\text{aux}}$ ) [35,44]. Assuming stoichiometric conditions and total recycling of solvents and catalysts,  $E_{\text{factor}}$  and RME are correlated. The carbon efficiency (CME) refers to the percentage of carbon in reactants that remains in the target product so that it will not be converted into emissions or waste [45]. Finally, the process mass intensity (PMI) shows the total mass of materials used to produce a specified mass of the product. Equations corresponding to each of the used metrics can

**Table 1**

Summary of experimental results over A15. Reaction conditions:  $T = 323\text{--}383\text{ K}$ ,  $R^{\circ}_{LA/1B} = 0.4\text{--}3.0$ , stirring speed = 750 rpm, initial reactants load  $\approx 2\text{ mol}$ , and catalyst load = 5 g of A15.

Run	T (K)	$x^{\circ}_{1B}$	$R^{\circ}_{LA/1B}$	$X_{1B}$ (%)	$X_{LA}$ (%)	$S^{SBL}_{1B}$ (%)	$S^{trans2B}_{1B}$ (%)	$S^{cis2B}_{1B}$ (%)	$S^{2BuOH}_{1B}$ (%)	$S^{SBL}_{LA}$ (%)	$Y^{SBL}_{1B}$ (%)	$Y^{SBL}_{LA}$ (%)
1	383	0.50	1.0	85.0	38.7	50.7	25.7	21.7	1.9	100	43.1	38.7
2	373	0.33	2.0	82.7	28.9	48.9	26.4	23.5	1.1	100	40.4	28.9
3	373	0.67	0.5	89.5	76.8	53.7	26.4	18.6	1.3	100	48.1	76.8
4	348	0.25	3.0	69.8	4.4	9.1	43.7	39.7	6.8	100	6.4	4.4
5 <sup>a</sup>	348	0.50	1.0	$73.5 \pm 1.4$	$19.2 \pm 1.9$	$30.9 \pm 2.1$	$35.2 \pm 0.5$	$27.5 \pm 0.6$	$3.1 \pm 0.5$	100	$23 \pm 2$	$19.2 \pm 1.9$
6	348	0.72	0.4	83.5	80.2	44.2	31.6	23.2	1.1	100	36.9	80.2
7 <sup>a</sup>	323	0.33	2.0	$53.0 \pm 1.6$	$0.74 \pm 0.12$	$3.2 \pm 0.5$	$46.8 \pm 0.2$	$47.3 \pm 0.4$	$2.8 \pm 0.2$	100	$1.7 \pm 0.3$	$0.74 \pm 0.12$
8	323	0.67	0.5	31.4	19.7	30.4	35.0	33.2	1.4	100	9.5	19.7

<sup>a</sup> Standard uncertainty is shown for replicated experiments

be found in Section D of the Supporting Information.

All mentioned metrics can be evaluated from different perspectives, i.e. complete reclaiming of catalysts and solvents, partial reclaiming, and no reclaiming whatsoever (the catalyst and solvents used are not recovered and reused). For the sake of comparison, only the no reclaiming and complete reclaiming scenarios have been assessed in the present work since they provide a glimpse of two opposite situations.

### 3. Results and discussion

#### 3.1. Conversion and selectivity

Fig. 1 shows the mole evolution of the main species detected for two typical experiments performed at 373 K and  $R^{\circ}_{LA/1B} = 2.0$  (Fig. 1-a) or  $R^{\circ}_{LA/1B} = 0.5$  (Fig. 1-b). As seen, 1-butene readily isomerizes to *cis*- and *trans*-2-butenes. This isomerization reaction would take place simultaneously to that of esterification with LA to produce SBL. From experimental observations, esterification of 2-butenes isomers with LA to produce SBL cannot be discarded, albeit lower reactivity can be expected from these olefins as compared to 1-butene due to more internal position of the double bond. Only minimal amounts of by-products were formed, namely olefin dimers due to the self-reactivity of butenes over acidic conditions (which, for the sake of clarity, are not shown in Fig. 1), and 2-butanol from olefin hydration due to the unavoidable remaining water in reactants and resin. Regarding the mechanism of ester formation at molecular level, it has been reported in the literature that the esterification of carboxylic acids with olefins proceeds by a two-step addition mechanism: i) the protonation of the olefin to form a secondary carbenium ion, and ii) the nucleophilic attack of the acid to the formed carbenium ion [46].

The screening of reaction conditions was always performed over 5 g of Amberlyst-15 (A15), without any solvent, and following the experimental design shown in Fig. S3 of the Supporting Information. Therefore, the initial mole fraction of 1-butene varied from 0.25 to 0.72 (which corresponds to  $R^{\circ}_{LA/1B}$  ranging from 3 to 0.4) and temperature from 313 K to 373 K. Unfortunately, quantification of the experiment at 313 K and  $R^{\circ}_{LA/1B} = 1.0$  could not be accomplished due to liquid phase separation along the circuit connecting reactor and GC/MS which, ultimately, led to inaccurate GC/MS readings. The formation of separate liquid phases had been already reported in a previous work [18]. The conversion, selectivity, and yield values for each experiment have been determined according to Eqs. S1 – S3 from reactor compositions as determined by GC–MS at a reaction time of 300 min (Table 1) since no further reaction progress was observed in longer experiments. These values reveal that the conversion of both 1-butene and levulinic acid increases with temperature. On the other hand, the effect of 1-butene concentration in the reactants mixture prompted different results. For instance, for experiments at 348 and 373 K, both 1-butene and levulinic acid conversions increase with increasing  $x^{\circ}_{1B}$  but, at lower temperatures ( $T = 323\text{ K}$ ), 1-butene conversion decreases with increasing  $x^{\circ}_{1B}$  from 0.33 to 0.67, whereas levulinic acid conversion increases.

Thus, within the assayed experimental conditions range, the best

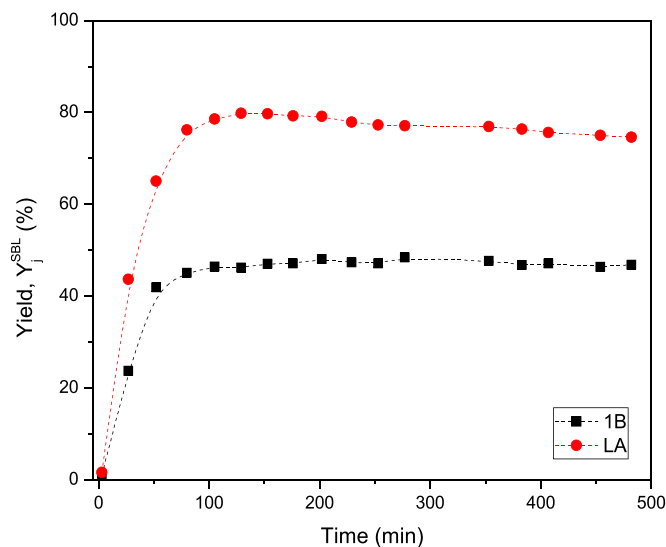


Fig. 2. Yield to *sec*-butyl levulinate with regards to 1-butene (1B) and levulinic acid (LA) over time at the best assayed conditions:  $T = 373\text{ K}$ ,  $R^{\circ}_{LA/1B} = 0.50$  (that is,  $x^{\circ}_{1B} = 0.67$ ), stirring speed = 750 rpm, initial reactants load  $\approx 2\text{ mol}$ , and catalyst load = 5 g of A15. Dashed lines are guides to the eye.

results were found at  $T = 373\text{ K}$  and  $R^{\circ}_{LA/1B} = 0.5$  (i.e.,  $x^{\circ}_{1B} = 0.67$ ), with yields to SBL with regards to 1-butene and levulinic acid of 48.1% and 76.8%, respectively. Notice that LA conversion can only be attributed to SBL formation whereas 1-butene consumption accounts for its participation in esterification, isomerization, hydration, and oligomerization reactions potentially taking place at the same time. Therefore, LA selectivity towards *sec*-butyl levulinate was considered as 100%. Fig. 2 shows the evolution of 1-butene and levulinic acid yields towards SBL with the course of an experimental run at those conditions.

With regards to 1-butene side reactions, 2-butanol and oligomeric compounds from side reactions of butene species were detected, though in low extension. As mentioned, the production of 2-butanol can be explained by the presence of water in the system, which causes the hydration of 1-butene. The water sources in the system are the unavoidable water remaining in the catalyst beads after drying, and the amount of water contained in the reactants (in particular, levulinic acid presented about 1% of water). In coherence with these facts, very low selectivity values of 1-butene to 2-butanol are observed.

Besides, positional double bond isomerization of 1-butene to *trans*-2-butene and *cis*-2-butene was the main side reaction observed at all experimental conditions, especially at low temperature. At these conditions, the equilibrium of isomerization reaction is shifted to the formation of 2-alkenes because the *trans*-2-butene is thermodynamically favored [47,48].

With regards to other byproducts, individual identification of every obtained byproduct in each experiment was not always possible due to

**Table 2**  
Statistical data analysis for coded regressors.

Variable	$Y_{1B}^{SBL}$			$Y_{LA}^{SBL}$		
Box-Cox transformation	$1 + (Y_{1B}^{SBL-0.051} - 1)/(-0.051 \cdot 13.94^{-1.05})$			$1 + (Y_{LA}^{SBL-0.049} - 1)/(0.049 \cdot 12.78^{-0.95})$		
Term	Coefficient	Standard uncertainty	p-value	Coefficient	Standard uncertainty	p-value
$\beta_0$	1.77	2.8	0.55	-13.0	1.7	0.0005
$\beta_1 (T)$	89	10	0.0003	89	6	$<10^{-4}$
$\beta_2 (x_{1B}^0)$	38	5	0.0006	56	3	$<10^{-5}$
$\beta_3 (T x_{1B}^0)$	-39	10	0.011	-45	6	0.0007
$\beta_4 (T^2)$	-34	10	0.016	-34	6	0.002
$F_{reg}$	74.6			276.6		
$R^2_{adjusted}$	0.970			0.992		

low side reactions extension in the explored conditions. For instance, the total chromatographic area for all byproducts detected ranged from 0.1 to 0.5% in the experiments performed. However, further analysis of obtained byproducts allowed identifying several branched C8 alkenes (such as 2,4-dimethyl-2-hexene, 3,5-dimethyl-2-hexene, 3,4-dimethyl-2-hexene, 3,4-dimethyl-3-hexene, and 3-ethyl-4-methyl-2-pentene), reasonably produced through dimerization and/or co-dimerization of 1-butene and 2-butenes, as well as di-*sec*-butyl ether, possibly produced through etherification of formed 2-butanol (see Figs. S4-S9 in Supporting Information for obtained MS spectra).

### 3.2. Response surface

To identify the optimal conditions to synthesize SBL employing the proposed reaction pathway, the yield of the desired product ( $Y_j^{SBL}$ ) with regards to both reactants was selected as the response variable of interest in multivariable analysis to obtain empirical equations that are subsequently optimized by overlaying the corresponding contour plots. This procedure should confirm and improve the results of the previous section by more accurate identification of optimal conditions. A response surface methodology analysis was adopted to find empirical equations able to describe the variation of responses with the relevant experimental conditions within the range explored. The factors considered were temperature and 1-butene molar fraction in the reactants mixture, and a second-order polynomial expression with interaction terms (Eq. 1) was fitted to experimental data through the stepwise procedure to account for those terms that exert a statistically significant influence on the response ( $p$ -value  $<0.05$ ). Since polynomials are empirical models, Box-Cox transformations of yield values, rather than actual yields, were used as response variables to enhance the normality

of data and because they provided a better fit. Furthermore, factors values were scaled to fit in the range of 0 to 1, to avoid possible biases in the statistical analysis due to their values being of considerably different magnitudes

Table 2 lists the parameter values, as well as their standard error and  $p$ -value, with the regression  $F$  statistic, and the adjusted  $R^2$  for the resulting best models, considering each reactant, when coded regressors are used. As indicated in Table 2, both  $\beta_1$  and  $\beta_2$  presented a positive effect on both response variables, as expected from data in Table 1, whereas  $\beta_3$  and  $\beta_4$  were negative. For both equations, the independent term  $\beta_0$  has been imposed, even though it was not significant for the 1-butene yield equation. In summary, a rise in reaction temperature and a larger amount of 1-butene enhances the yields towards the desired ester, but as the temperature keeps rising, a drop in yields is observed

The derived expressions, in terms of uncoded regressors, are:

$$Y_{1B}^{SBL} = \left[ \left[ (1.6 \pm 0.3) \cdot 10^3 - (8.0 \pm 1.9)T - (0.53 \pm 0.12) \cdot 10^3 x_{1B}^0 + (1.4 \pm 0.4)T x_{1B}^0 + (0.010 \pm 0.003)T^2 + 1 \right] \cdot 0.051 \cdot 13.94^{-1.05} + 1 \right]^{-\left(\frac{1}{0.051}\right)} \quad (2)$$

$$Y_{LA}^{SBL} = \left[ \left[ -(1.6 \pm 0.2) \cdot 10^3 - (8.0 \pm 1.1)T - (0.64 \pm 0.07) \cdot 10^3 x_{1B}^0 + (1.6 \pm 0.2)T x_{1B}^0 + (0.0095 \pm 0.0016)T^2 - 1 \right] \cdot 0.049 \cdot 12.78^{-0.95} + 1 \right]^{-\left(\frac{1}{0.049}\right)} \quad (3)$$

where  $Y_j^{SBL}$  is the yield of reactant  $j$  towards SBL in percentage,  $x_{1B}^0$  is expressed in parts per unit, and  $T$  in K. As shown in Fig. 3a, values predicted by Eqs. (2) and (3) fit remarkably well with observed

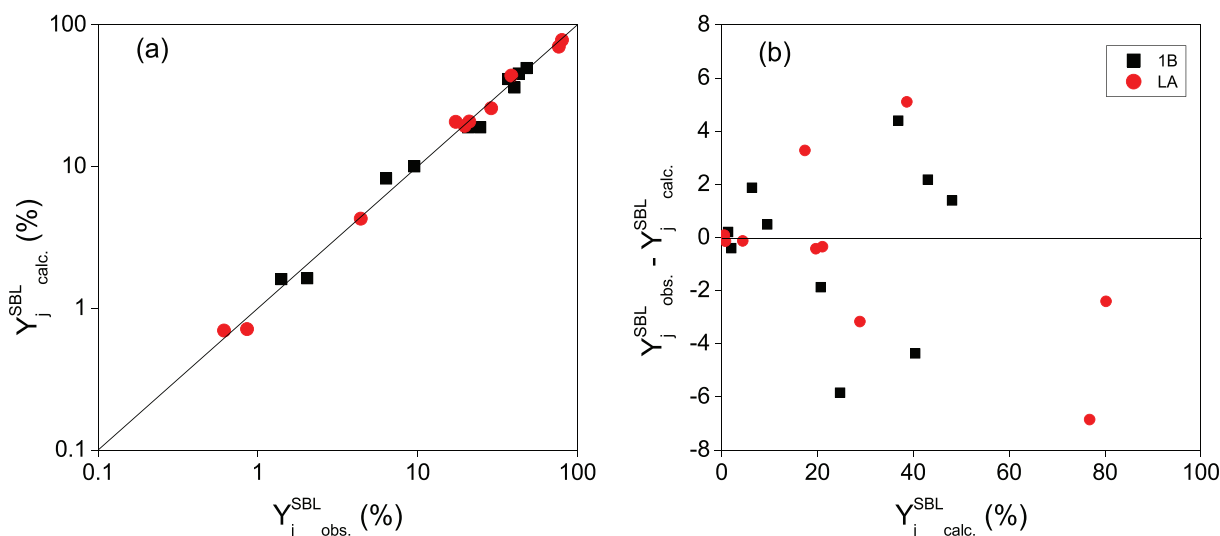


**Fig. 3.** Comparison between observed and calculated yield values (a), and residuals distribution (b).

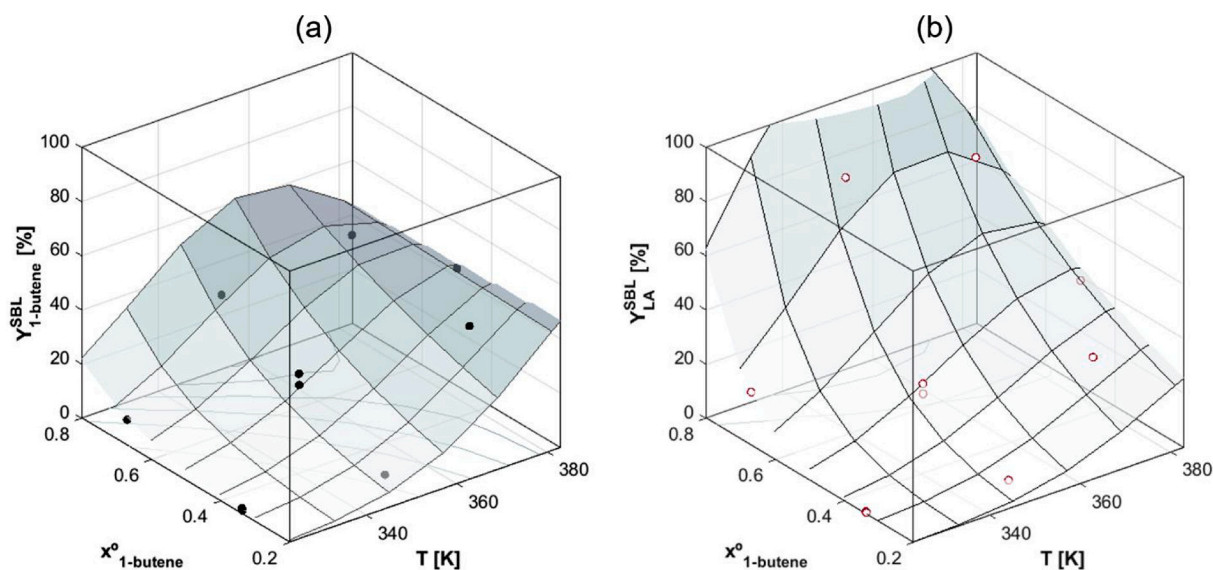


Fig. 4. Response surfaces for (a) 1-butene and (b) levulinic acid yields towards sec-butyl levulinate.  $Y_{1B}^{SBL}$  (●) and  $Y_{LA}^{SBL}$  (○).

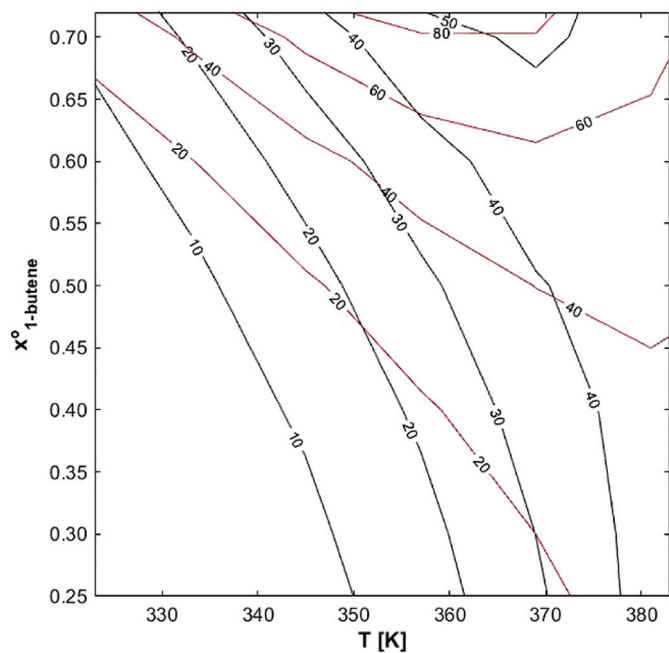


Fig. 5. Overlaid contour plots for 1-butene and levulinic acid yields towards sec-butyl levulinate.  $Y_{1B}^{SBL}$  (—) and  $Y_{LA}^{SBL}$  (—).

experimental results. Fig. 3b shows distribution of residuals to provide further details regarding the goodness of the fit.

As illustrated in Fig. 4, the shape of the response surface is globally similar for both reactants but the enhancing effect on yields of high 1-butene initial content is considerably more pronounced for levulinic acid than for 1-butene. As two different reaction yields are evaluated from the experimental data, a multiobjective optimization (MOO) is necessary to highlight optimum reaction conditions. Overlaying contour plots is a straightforward MOO approach that allows for pinpointing such conditions at a glance. Thereby, Fig. 5 better illustrates operating conditions that favor yields from both reactants to SBL. As seen, a large concentration of 1-butene in the composition of reactants as well as high temperature favor both yields, and the optimal temperature can be identified between 360 and 370 K.

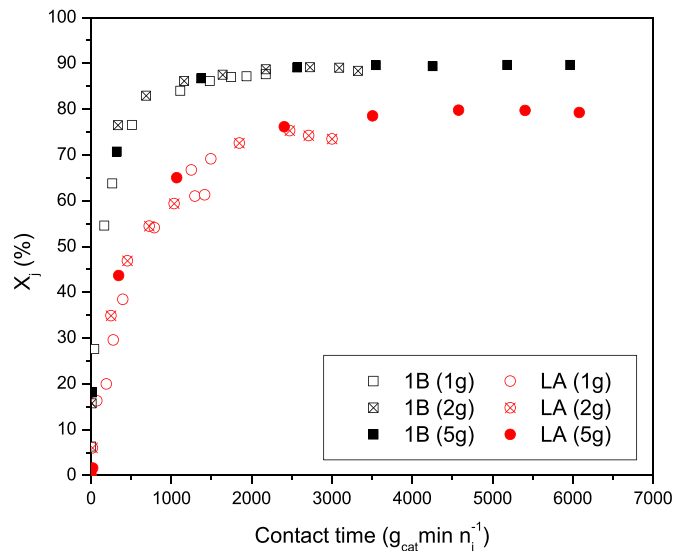


Fig. 6. Evolution of reactants conversion with respect to the contact time for different catalyst (A15) loads. Reaction conditions:  $T = 373$  K,  $R^{LA/1B} = 0.5$ , stirring speed = 750 rpm, initial reactants load  $\approx 2$  mol.

### 3.3. Effect of the catalyst load

The effect of the catalyst load was evaluated at  $R^{LA/1B} = 0.50$  ( $x^{1B} = 0.67$ ) and 373 K, with a stirring speed of 750 rpm, and initial reactants load to the reactor of about 2 mol. Explored catalyst (A15) amounts were 1, 2 and 5 g. Fig. 6 depicts the obtained reactants conversion for the different catalyst loads as a function of contact time, which is a standardized time that can be used to compare experiments. Since the obtained patterns for the different catalyst loads overlap, it can be concluded that the effect of catalyst loads up to 5 g of catalyst is negligible under the explored experimental conditions.

With respect to side reactions extension in these experiments, obtained results revealed close to null differences under assayed reaction conditions. Together, the produced amounts of 2-butanol and all detected oligomeric compounds added up to about 1–1.5% of the total chromatographic area regardless of the catalyst load at the end of each run, which reinforces the choice of present reaction conditions as the

**Table 3**

Physical and morphological properties of A15, A16, A39, A46, CT175, and Dow2, as well as obtained experimental results for catalytic activity tests.

	A15	A16	A39	A46	CT175	Dow2
General characteristics						
Structure	Macro-reticular	Macro-reticular	Macro-reticular	Macro-reticular	Macro-reticular	Micro-reticular
Divinylbenzene [%]	20	12	8	20	20	2
Skeletal density, $\rho^a$ [g/cm <sup>3</sup> ]	1.416	1.401	1.417	1.137	1.498	1.426
Acid Capacity <sup>b</sup> [meq H <sup>+</sup> /g]	4.81	4.8	4.81	0.87	4.98	5.06
Mean particle diameter, $d_{p,m}^c$ [ $\mu$ m]	650.1	562.5	540	775.5	940	252
Dry state properties: adsorption-desorption of N <sub>2</sub> at 77 K <sup>d</sup>						
BET surface area, $S_{BET}^e$ [m <sup>2</sup> /g]	42.0	1.69	0.09	57.4	28	1.32
Pore volume, $V_g^f$ [cm <sup>3</sup> /g]	0.328	0.013	0.0003	0.263	0.3	0
Mean pore diameter, $d_{m,pore}^g$ [nm]	31.8	29.7	17.6	19.2	45.1	0
Swollen in water morphology: ISEC method <sup>h</sup>						
Macro-mesopore surface area, $S_{area}$ [m <sup>2</sup> /g]	192	46.2	56.1	186	90.7	0
Macro-mesopore pore volume, $V_{pore}$ [cm <sup>3</sup> /g]	0.616	0.188	0.155	0.47	0.615	0
Macro-mesopore mean pore diameter, $d_{pore}^g$ [nm]	12.8	16.3	11.1	10.1	32.7	0
Gel-phase volume of the swollen polymer phase, $V_{sp}$ [cm <sup>3</sup> /g]	0.765	1.129	1.624	0.523	0.908	2.655
Catalytic activity test results <sup>i</sup>						
SBL initial formation rate, $r_{SBL}^j$ [mol/(g·h)]	0.169	0.135	0.048 ± 0.006	0.030	0.11 ± 0.02	0.016 ± 0.005
Yield to 2-butanol, $Y_{IB}^{2BuOH}^j, k$ [%]	1.2	2.2	2.0 ± 0.8	0.4	2.3 ± 0.4	2.23 ± 0.07

<sup>a</sup> Skeletal density. Measured by Helium displacement (Accupic 1330).

<sup>b</sup> Titration against the standard base.

<sup>c</sup> Laser diffraction technique in air.

<sup>d</sup> Samples dried at vacuum (0.001 MPa, 383 K).

<sup>e</sup> BET method (Brunauer-Emmett-Teller).

<sup>f</sup> Volume of N<sub>2</sub> adsorbed at a relative pressure ( $P/P_0$ ) = 0.99.

<sup>g</sup>  $d_{m,pore} = 4V_g/S_g$  or  $d_{pore} = 4V_{pore}/S_{area}$ , respectively.

<sup>h</sup> Inverse Steric Exclusion Chromatography technique [49,50].

<sup>i</sup> Experimental conditions were T = 373 K, P = 2.5 MPa,  $R_{LA/1B}^o = 0.5$ , and 2 g of catalyst.

<sup>j</sup> Typical error is shown for replicated experiments.

<sup>k</sup> Yield to 2-butanol with regards 1-butene at 50% 1-butene conversion.

optimum ones for the production of *sec*-butyl levulinate.

### 3.4. Catalysts screening

Aiming to rationalize the relations between catalytic activity and resins morphological properties, a set of commercially available resins with similar acid capacity and different crosslinking degree (%DVB, Table 3) was tested at optimal operating conditions, that is at T = 373 K, P = 2.5 MPa, and  $R_{LA/1B}^o = 0.5$ , with a catalyst load of 2 g. A46 is an exception because it presents structural properties similar to those of A15 but much lower acid capacity (0.87 meqH<sup>+</sup>/g<sub>cat</sub>) than the other resins.

Catalytic activity results, also shown in Table 3, were expressed in terms of initial SBL formation rate ( $r_{SBL}^o$ ). Initial reaction rates (Eq. S4 in Supporting Information) are a direct indication of the activity level achieved by a catalyst under the same reaction conditions, that is in absence of reaction products. As seen in Table 3, significant differences in the catalytic activity levels displayed by the tested resins were observed. As expected, A46 presented the lowest activity, which is in agreement with its low number of active sites. On the contrary, A15 was the most active catalyst, followed by A16, CT175, A39, and Dow2. Since almost no differences exist between the acid capacities of these catalysts, it is reasonable to assume that the observed activity differences arise from their different structural properties.

It is to be noted that properties like BET surface area and pore volume, very useful for explaining behavior for other types of catalysts [6], appear to be inadequate to explain catalytic activity rank observed in this work. This fact is related to resins capability to swell when immersed in polar media, which results in textural parameters obtained in “dry” conditions (that is, in absence of solvents) being non-representative of the actual catalysts working-state conditions during reaction [51–53]. As a solution to circumvent this drawback, textural parameters of resins immersed in water, a strong polar medium, can be

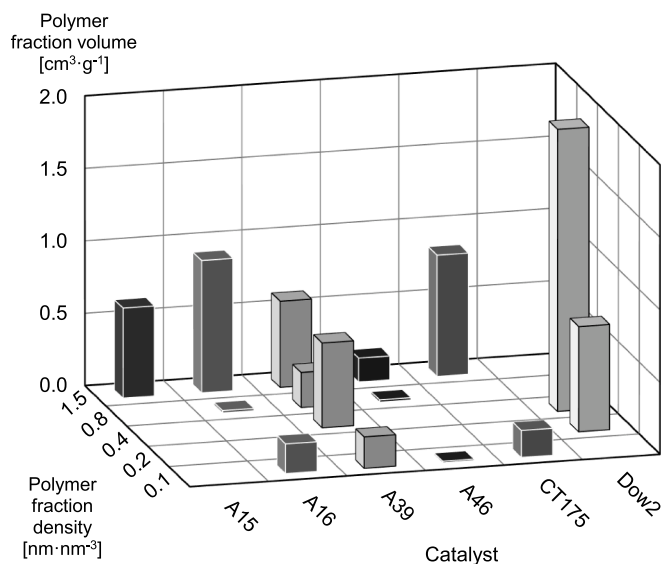
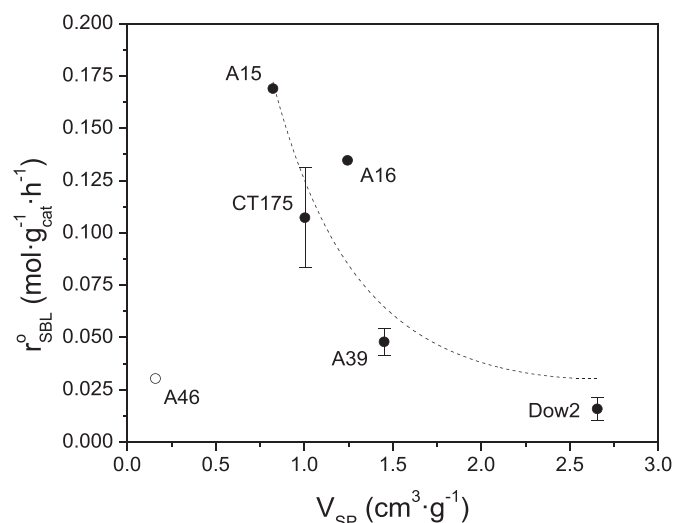


Fig. 7. ISEC morphological pattern of the gel-type phase for tested resins.

obtained by Inverse Steric Exclusion Chromatography (ISEC). This alternative characterization provides information about the macro- and micropore domains of the resins in a swelling state [49,50]. As shown in Fig. 7, ISEC analysis allows obtaining morphological patterns to identify individual polymer volume fractions in the resins gel-type phase, which are characterized by the polymer density in each fraction. As seen in the figure, gel phase of resins A15, A16, A46, and CT175 is mainly distributed in the densest polymer fraction (i.e., 1.5 nm<sup>3</sup>/nm<sup>3</sup>) with little or null contribution of lighter fractions, whereas less dense polymer domains



**Fig. 8.** Initial SBL formation rates against  $V_{SP}$  for experiments at  $T = 373$  K and  $R_{LA/1B} = 0.5$  performed with A46 (○) and with resins with a similar number of active sites (●). Error bars refer to typical error for replicated experiments. The dashed line is a guide to the eye.

**Table 4**

Length ( $d_m$ ) of reactants and main product, Ogston distribution coefficients ( $K_O$ ) in different domains of swollen polymers with density  $C$ , and respective equivalent pore size.

Compound	$d_m$ (nm) <sup>a</sup>	Ogston distribution parameter, $K_O$ <sup>b</sup>				
Levulinic acid	0.66	0.92	0.84	0.70	0.49	0.27
1-butene	0.56	0.93	0.87	0.75	0.56	0.34
sec-butyl levulinate	1.30	0.80	0.64	0.40	0.16	0.03
Polymer chain density, $C$ (nm/nm <sup>3</sup> ) <sup>c</sup>		0.1	0.2	0.4	0.8	1.5
Equivalent pore size (nm) <sup>d</sup>		9.3	4.8	2.6	1.5	1.0

<sup>a</sup> Estimated in the conformation of minimum energy by ChemBioOffice 19.0 software.

<sup>b</sup> Calculated according to Eq. S5 [49,52].

<sup>c</sup> From [49,50].

<sup>d</sup> From [52].

are more predominant in the gel-type phases of resins A39 and Dow2, which were the least active catalysts besides A46. This results would indicate that denser polymer domains favor the SBL formation reaction.

In fact, with regards to the relationship between ISEC features and observed catalytic activity, Fig. 8 depicts the initial SBL formation rates versus the total volume of swollen-polymer ( $V_{SP}$ ), which is the main characteristic parameter obtained by ISEC and accounts for the swelling of the resins gel-type phase, regardless of the density of each individual polymer fraction. As aforementioned, A46 (shown as an open symbol in Fig. 8), can be considered an exception, since all other resins tested in

**Table 5**

Green metrics for the different scenarios evaluated. No reclaiming perspective

Ref.	T (K)	Catalyst	Alkylating agent	$R_{LA/X}$ <sup>a</sup>	Solvent	AE	MRP	RME	Y <sup>b</sup>	1/SF	VMR	$E_{factor}$ <sup>c</sup>	$E_{aux}$	CME
This work	373	A15	1-butene	0.50	–	1.00	0.97	0.55	0.77	0.74	0.82	0.66	0.06	51.69
[18]	373	A15	1-butene	0.33	–	1.00	0.99	0.12	0.21	0.56	0.69	7.57	0.06	11.01
[18]	373	H <sub>2</sub> SO <sub>4</sub>	1-butene	0.33	–	1.00	0.98	0.29	0.50	0.60	0.73	2.33	0.07	26.20
[18]	373	A15	1-butene	0.05	$\gamma$ -butyro-lactone	1.00	0.09	0.01	0.66	0.54	0.54	9.83	115.5	7.03
[55]	513	Zr(SO <sub>4</sub> ) <sub>2</sub> ·4H <sub>2</sub> O	2-butanol	0.05	–	0.91	0.99	0.06	0.74	0.08	0.69	17.28	0.14	5.39
[56] <sup>d</sup>	523	WO <sub>3</sub> -SBA-16	2-butanol	0.14	–	0.91	0.99	0.03	0.13	0.28	0.62	29.50	0.14	3.55

<sup>a</sup> Refers to the molar ratio of levulinic acid to the alkylating agent (X).

<sup>b</sup> In all the cases the yield of acid to the corresponding butyl levulinate has been considered except for the last entry in the table, where the yield of 1-butanol to butyl levulinate is evaluated.

<sup>c</sup> The  $E$ -factor considered equals the PMI-1 and does not account for the use of auxiliary materials as solvent and catalyst that are accounted for in the  $E_{aux}$ .

<sup>d</sup> Calculated on basis of 100 g of feed

the present work present a similar acid capacity. The overall picture reveals that the resins catalytic activity decreases as the volume of the gel phase increases, which for similar acid capacity values is related to lower density of active sites. Therefore, resins with a larger concentration of active sites per unit volume boost the formation of SBL. This suggests that multiple active sites could coordinate to better accommodate reactants, promoting thereby the formation of hydrogen bonded intermediates that eventually favor the SBL formation reaction.

On the other hand, accessibility of the relatively large molecules LA and SBL to the different domains of the polymer network for every catalyst can be estimated by Ogston distribution coefficients,  $K_O$  (shown in Table 4 and calculated by Eq. S5 of the Supporting Information), which allow quantification of the ease of penetration of a molecule into a porous domain of a certain density in relation to its quantity in the free solution [49,52].

As seen in Table 4, none of the involved compounds presents free access to every polymer domain, which suggests that active sites located in internal parts of the catalyst gel phase might be inaccessible to reactants, hence ineffective for the present reaction. This could lead to assuming that the reaction would take place mainly on the outer shell of the catalysts gel phase and, consequently, resins with larger specific surface should present higher activity because this would grant reactants easier access to active sites. In fact, the most active catalyst, i.e. A15, presents the highest specific surface in swollen-state conditions among the tested resins (Table 3, 192 m<sup>2</sup>/g). However, this assumption seems to contradict A39 and A16 results, which showed very different activity levels (0.048 mol·g<sup>-1</sup>·h<sup>-1</sup> and 0.135 mol·g<sup>-1</sup>·h<sup>-1</sup>, respectively) and have almost the same specific surface (56.1 m<sup>2</sup>/g and 46.2 m<sup>2</sup>/g, respectively). As previously mentioned, the different activity levels displayed by these two catalysts can be explained by the higher polymer density of A16 gel-type phase (Fig. 7), which entails shorter distances between active sites in the resin and, therefore, reinforce the idea that denser distributions of active sites favor multiple coordination with reactants.

Therefore, present results would indicate that two morphological characteristics, that is gel-type phase density and specific surface in swollen-state conditions, play a role in the observed activity rank for tested ion-exchange resins. Resins with dense polymer fraction distribution of gel-type phase and large specific surface would allow reactants access to polymer domains with high concentration of active sites, which would in turn promote multiple coordination and, consequently, boost SBL formation. The fact that A46 presented similar activity levels from A39 and Dow2 with much lower number of active sites is considered an empirical evidence for the two effects described, since A46 presents very large specific surface in swollen-state conditions and its gel-type phase is mainly distributed in dense polymer fractions.

Finally, regarding the side reactions extension in the catalyst screening experiments, a comparison of the byproducts formed at the end of experiments is not straightforward because the conversion at the same contact time was significantly different for each catalyst. Instead, a proper comparison of the yield to the main byproduct obtained, -i.e. 2-

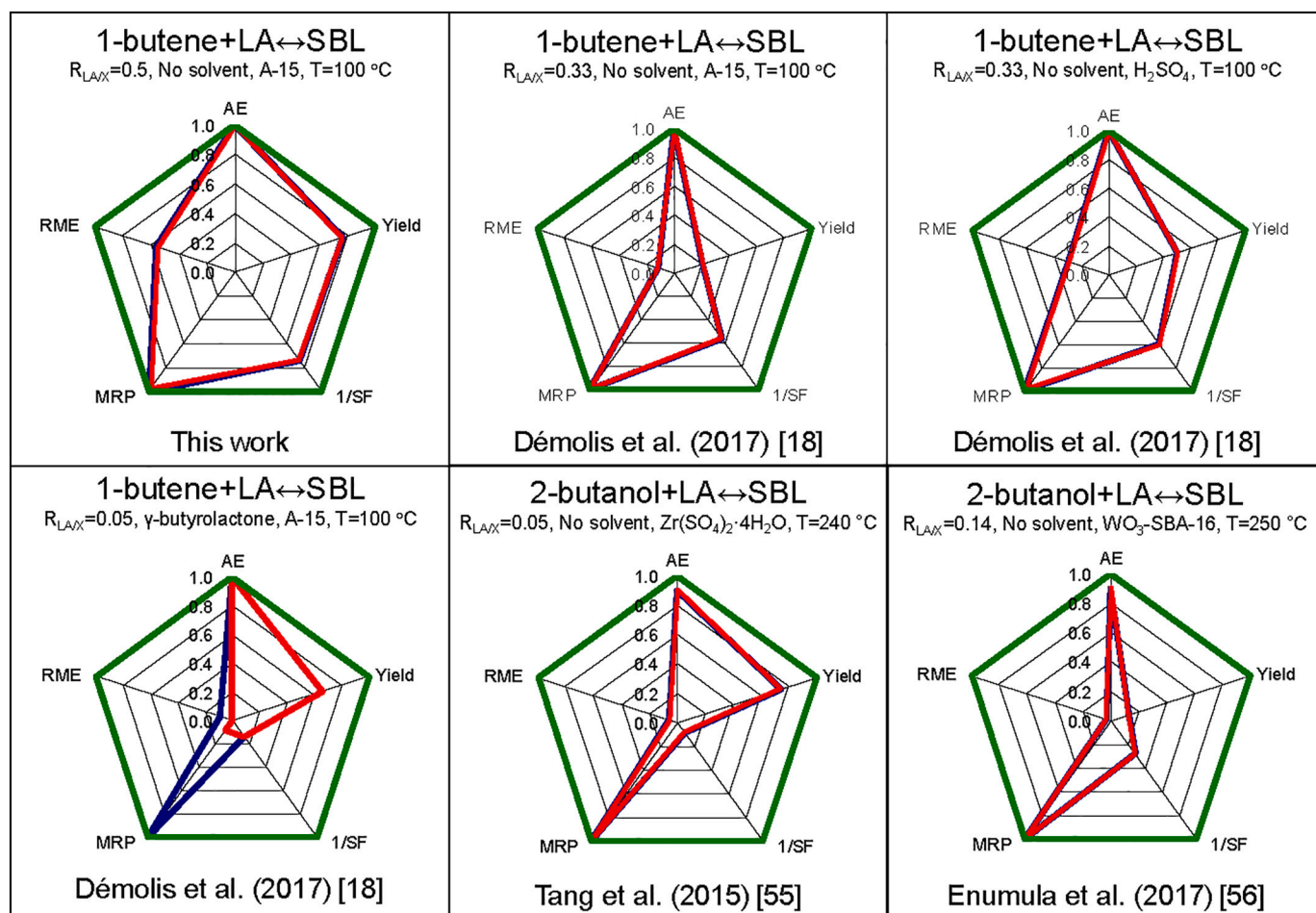


Fig. 9. Radial pentagons resulting from the green metrics analysis of the syntheses evaluated in Table 3 under complete reclaiming (blue) and no reclaiming (red) approaches. Green series refer to the ideal. Please note that in most of the cases blue and red series are overlapped.

butanol, can be evaluated at a constant 1-butene conversion of 50%. This value was chosen as reference because it was the lowest conversion reported, corresponding to that obtained with A46. Table 3 also provides such comparison, where little differences are observed for most of the catalysts evaluated. It is however to be noted that A46 and A15 presented lower 2-butanol formation (0.4 and 1.2%, respectively) than the rest of resins. In the case of A46, its low number of active sites can explain its low catalytic activity towards both SBL and byproducts. For A15, the low extension of side-reactions together with its higher catalytic activity, highlight this resin as the best possible catalyst evaluated. Interestingly, A15 was also identified as an excellent catalyst in a recent study [54] focusing the synthesis of linear levulinates from LA and ethanol.

### 3.5. Green metrics evaluation

Two main routes of *sec*-butyl levulinate synthesis have been considered in the GMA performed: (i) 1-butene as the esterifying agent and, (ii) 2-butanol as the alkylating agent. According to this classification, the data extracted from several studies recently reported in the literature are used for comparison of metrics. Also, the use of solvents in case (i) has been assessed. Table 5 summarizes the main results obtained in terms of the metrics evaluated for the no reclaiming approach and Fig. 9 illustrates the corresponding radial pentagons for each case evaluated under complete and no reclaiming scenarios.

From Table 5 values and Fig. 9 diagrams emerge that the chemical pathway studied in this work for the production of *sec*-butyl levulinate under the reactants molar ratios used is the greenest alternative among

the different scenarios evaluated. Noteworthy, our values differ significantly from those reported by Démolis [18] using a higher molar ratio LA/olefin of 0.33 yet under identical reaction temperature using A15 (second entry). At these conditions, a lower yield is also reported using H<sub>2</sub>SO<sub>4</sub> as catalyst (third entry) despite the interesting overall metric values. The use of a homogeneous catalyst, viz. difficulty of separation and reuse, is however another setback to be considered. As expected, the use of reactants in non-stoichiometric amounts implies negative aftermath on the SF and RME. On the other hand, the use of  $\gamma$ -butyrolactone (fourth entry) allowed for increasing the reaction yield from 0.21 (second entry) to 0.66 but again, the low  $R_{LA/X} = 0.05$  used is far from the stoichiometric and lessens the RME and SF metrics [57]. Also, the use of solvent presents an important detrimental effect of MRP under no-reclaiming conditions to consider.

Regarding the scenario considering the use of 2-butanol as the alkylating agent, as a whole, the process is less attractive due to the lower atom economy derived from the by-production of water and the higher reaction temperatures usually applied (Fig. 9). Moreover, the used non-stoichiometric LA:alcohol molar ratios result in very low RME and SF metrics that reduces significantly the greenness of these approaches in comparison to the results reported at the best experimental conditions in the present work. Similar conclusions can be drawn from the analysis of the  $E_{\text{factor}}$  and CME metrics, which globally are affected by the use of excess reactants and by-products formation.

The performed green metrics analysis reflects that not only the reaction yield to target products must be considered when designing possible synthetic routes for a process. Very often, this is the only process variable to which the entire heed is paid towards optimization when

evaluating new catalysts or new synthetic routes. However, limiting the use of excess reactants and restricting the use of solvents must also be targeted for designing greener efficient processes. Besides, the use of bio-based reactants when possible is essential for driving the production of the fuels towards a greener and more sustainable industry

#### 4. Conclusions

The feasibility of the proposed chemical reaction pathway is strongly supported by the low amount of formed byproducts, which is the main drawback of the conventional synthesis of butyl levulinates. The best results in terms of maximum yield to the desired ester with regards to both reactants are observed at 373 K and with an excess of 1-butene in the reactants mixture ( $x_{1B}^{\circ} = 0.67$ , or  $R_{LA/1B}^{\circ} = 0.5$ ), with yields of 48.1% for 1-butene and 76.8% for levulinic acid. Also, empirical relationships between operating conditions and SBL yields have been obtained through a stepwise multivariate regression procedure, allowing accurate prediction of yield values within assayed conditions. Furthermore, a response surface methodology analysis and subsequent multiobjective optimization identified optimal conditions that maximize simultaneously the yield of the two reactants to *sec*-butyl levulinate, which correspond to high 1-butene initial concentration and temperature in the range 360–370 K. With regards to catalyst load, no significant effects on conversions have been detected for catalyst loads ranging from 1 to 5 g of catalyst, which corresponds to 0.6–3.1%wt. in the reactor vessel. Thanks to the catalysts screening, it has been pointed out that narrow micropore-sized cavities in ion-exchange resins gel phase and large specific surface in swollen-state conditions favor access of reactants to polymer domains with high density of active sites, which promote multiple active sites coordination with reactants and boost SBL formation. Among the tested resins, A15 has been identified as the most attractive catalyst due to low extension of side-reactions and high catalytic activity. The green metrics analysis reveals that the proposed synthesis pathway is the greenest alternative to obtain *sec*-butyl levulinate among the analyzed synthesis plans, and therefore the most attractive option for industrial exploitation from an environmental standpoint. The high conversions and yields at relatively low temperature and molar ratios close to the stoichiometric ones make the inexpensive and green catalyst A15 a promising candidate for the synthesis of *sec*-butyl levulinate in the absence of solvents. From a future perspective, a reusability study of ion-exchange resins as catalysts could be useful to elucidate the potential industrial implementation of the studied reaction pathway

#### Declaration of Competing Interest

The authors declare that they have no known competing financial interests or personal relationships that could have appeared to influence the work reported in this paper.

The authors declare the following financial interests/personal relationships which may be considered as potential competing interests:

#### Acknowledgments

The authors are grateful to MINECO (CTQ2017-84398-R Grant) for their financial support and to Dow Water & Process Solutions for providing ion exchange resin samples.

#### Appendix A. Supplementary data

Supporting Information of this article can be found online at <https://doi.org/10.1016/j.fuproc.2021.106893>.

#### References

- [1] J. Rogelj, N. den Elzen, N. Höhne, T. Fransen, H. Fekete, H. Winkler, R. Schaeffer, F. Sha, K. Riahi, M. Meinshausen, Paris agreement climate proposals need a boost to keep warming well below 2°C, *Nature* 534 (2016) 631–639, <https://doi.org/10.1038/nature18307>.
- [2] G. Berndes, M. Hoogwijk, R. van den Broek, The Contribution of Biomass in the Future Global Energy Supply: a review of 17 Studies, *Biomass Bioenergy* 25 (2003) 1–28, [https://doi.org/10.1016/S0961-9534\(02\)00185-X](https://doi.org/10.1016/S0961-9534(02)00185-X).
- [3] A.K. Agarwal, Biofuels (Alcohols and biodiesel) applications as Fuels for Internal Combustion Engines, *Prog. Energ. Combust.* 33 (2007) 233–271, <https://doi.org/10.1016/j.pecc.2006.08.003>.
- [4] S.N. Naik, V.V. Goud, P.K. Rout, A.K. Dalai, Production of first and Second Generation Biofuels: a Comprehensive Review, *Renew. Sust. Energ. Rev.* 14 (2010) 578–597, <https://doi.org/10.1016/j.rser.2009.10.003>.
- [5] A. Ben Hassen Trabelsi, K. Zaafouri, W. Baghdadi, S. Naoui, A. Ouergh, Second generation biofuels production from waste cooking oil via pyrolysis process, *Renew. Energy* 126 (2018) 888–896, <https://doi.org/10.1016/j.renene.2018.04.002>.
- [6] M.M. Zainol, M. Asmadi, P. Iskandar, W.A.N. Wan Ahmad, N.A.S. Amin, T.T. Hoe, Ethyl levulinate synthesis from biomass derivative chemicals using iron doped sulfonated carbon cryogel catalyst, *J. Clean. Prod.* 281 (2021) 124686, <https://doi.org/10.1016/j.jclepro.2020.124686>.
- [7] C.R. Carere, R. Sparling, N. Cicek, D.B. Levin, Third Generation Biofuels via Direct Cellulose Fermentation, *Int. J. Mol. Sci.* 9 (2008) 1342–1360, <https://doi.org/10.3390/ijms9071342>.
- [8] J. Lü, C. Sheahan, P. Fu, Metabolic Engineering of Algae for fourth Generation Biofuels Production, *Energy Environ. Sci.* 4 (2011) 2451–2466, <https://doi.org/10.1039/c0ee00593b>.
- [9] K. Yan, C. Jarvis, J. Gu, Y. Yan, Production and catalytic transformation of levulinic acid: a platform for specialty chemicals and fuels, *Renew. Sust. Energ. Rev.* 51 (2015) 986–997, <https://doi.org/10.1016/j.rser.2015.07.021>.
- [10] D.W. Rackemann, W.O.S. Doherty, The Conversion of Lignocellulosics to Levulinic Acid, *Biofuels Bioprod. Biorefin.* 5 (2011) 198–214, <https://doi.org/10.1002/bbb.267>.
- [11] P.A. Son, S. Nishimura, K. Ebitani, Synthesis of levulinic acid from fructose using Amberlyst-15 as a solid acid catalyst, *React. Kinet. Mech. Catal.* 106 (1) (2012) 185–192, <https://doi.org/10.1007/s11144-012-0429-1>.
- [12] Production of levulinic acid from carbohydrate-containing materials, 1997, U.S. Patent 5,608,105.
- [13] A. Morone, M. Apte, R.A. Pandey, Levulinic acid production from renewable waste resources: Bottlenecks, potential remedies, advancements and applications, *Renew. Sust. Energ. Rev.* 51 (2015) 548–565, <https://doi.org/10.1016/j.rser.2015.06.032>.
- [14] G.C. Hayes, C.R. Becer, Levulinic acid: a sustainable platform chemical for novel polymer architectures, *Polym. Chem.* 11 (2020) 4068–4077, <https://doi.org/10.1039/D0PY00705F>.
- [15] A. Démolis, N. Essayem, F. Rataboul, Synthesis and applications of Alkyl Levulinates, *ACS Sustain. Chem. Eng.* 2 (2014) 1338–1352, <https://doi.org/10.1021/sc500082n>.
- [16] S. An, D. Song, B. Lu, X. Yang, Y. Guo, Morphology Tailoring of Sulfonic Acid Functionalized Organosilica Nanohybrids for the Synthesis of Biomass-Derived Alkyl Levulinates, *Chem-Eur J.* 21 (2015) 10786–10798, <https://doi.org/10.1002/chem.201501219>.
- [17] J.A. Meleró, G. Morales, J. Iglesias, M. Paniagua, B. Hernández, D. Penedo, Efficient conversion of Levulinic Acid into Alkyl Levulinates Catalyzed by Sulfonic Mesoporous Silicas, *Appl. Catal. A-Gen.* 466 (2013) 116–122, <https://doi.org/10.1016/j.apcata.2013.06.035>.
- [18] A. Démolis, M. Eternot, N. Essayem, F. Rataboul, New insights into the reactivity of biomass with butenes for the synthesis of Butyl Levulinates, *ChemSusChem* 10 (2017) 2612–2617, <https://doi.org/10.1002/cssc.201700416>.
- [19] Preparation of Levulinic Acid Esters and Formic Acid Esters from Biomass and Olefins, 2003, US Patent 7,153,996-B2.
- [20] Preparation of Levulinic Acid Esters and Formic Acid Esters from Biomass and Olefins, 2005, US Patent 2005/0118691-A1.
- [21] Production of Levulinic Acid and Levulinate Esters from Biomass, 2010, US Patent 2010/0312006-A1.
- [22] K.C. Badgujar, V.C. Badgujar, B.M. Bhanage, A review on catalytic synthesis of energy-rich fuel additive levulinate compounds from biomass-derived levulinic acid, *Fuel Process. Technol.* 197 (2020) 106213, <https://doi.org/10.1016/j.fuproc.2019.106213>.
- [23] E. Christensen, A. Williams, S. Paul, S. Burton, R.L. McCormick, Properties and Performance of Levulinate Esters as Diesel Blend Components, *Energy Fuel* 25 (2011) 5422–5428, <https://doi.org/10.1021/ef201229j>.
- [24] J. Lange, W.D. van de Graaf, R.J. Haan, Conversion of furfuryl alcohol into ethyl levulinate using solid acid catalysts, *ChemSusChem* 2 (2009) 437–441, <https://doi.org/10.1002/cssc.200800216>.
- [25] H. Joshi, B.R. Moser, J. Toler, W.F. Smith, T. Walker, Ethyl Levulinate: a potential Bio-based Diluent for biodiesel which Improves Cold Flow Properties, *Biomass Bioenergy* 35 (2011) 3262–3266, <https://doi.org/10.1016/j.biombioe.2011.04.020>.
- [26] K.Y. Nandiwale, V.V. Bokade, Esterification of Renewable Levulinic Acid to n-Butyl Levulinate over Modified H-ZSM-5, *Chem. Eng. Technol.* 38 (2015) 246–252, <https://doi.org/10.1002/ceat.201400326>.
- [27] P.D. Carà, R. Ciriminna, N.R. Shiju, G. Rothenberg, Enhanced Heterogeneous Catalytic Conversion of Furfuryl Alcohol into Butyl Levulinate, *ChemSusChem* 7 (2014) 835–840, <https://doi.org/10.1002/cssc.201301027>.

- [28] Preparation of Tertiary Alkyl Levulinates, 1970, U.S. Patent 3,489,795.
- [29] E.I. Gürbüz, D.M. Alonso, J.Q. Bond, J.A. Dumesic, Reactive Extraction of Levulinic Esters and Conversion to  $\gamma$ -Valerolactone for production of Liquid Fuels, *ChemSusChem* 4 (2011) 357–361, <https://doi.org/10.1002/cssc.201000396>.
- [30] J. Gu, J. Zhang, D. Li, H. Yuan, Y. Chen, Hyper-cross-linked polymer based carbonaceous materials as efficient catalysts for ethyl levulinate production from carbohydrates, *J. Chem. Technol. Biotechnol.* 94 (2019) 3073–3083, <https://doi.org/10.1002/jctb.6107>.
- [31] Y. Tian, R. Zhang, W. Zhao, S. Wen, Y. Xiang, X. Liu, A New Sulfonic Acid-Functionalized Organic Polymer Catalyst for the Synthesis of Biomass-Derived Alkyl Levulinates, *Catal. Lett.* 150 (2020) 3553–3560, <https://doi.org/10.1007/s10562-020-03253-5>.
- [32] M.A. Harmer, Sun Q. Qun, Solid acid catalysis using Ion-Exchange Resins, *Appl. Catal. A-Gen.* 221 (2001) 45–62, [https://doi.org/10.1016/S0926-860X\(01\)00794-3](https://doi.org/10.1016/S0926-860X(01)00794-3).
- [33] E. Ramírez, R. Bringué, C. Fité, M. Iborra, J. Tejero, F. Cunill, Role of ion-exchange resins as catalyst in the reaction-network of transformation of biomass into biofuels, *J. Chem. Technol. Biotechnol.* 92 (2017) 2775–2786, <https://doi.org/10.1002/jctb.5352>.
- [34] J.H. Badia, C. Fité, R. Bringué, E. Ramírez, M. Iborra, Relevant properties for catalytic activity of sulfonic ion-exchange resins in etherification of isobutene with linear primary alcohols, *J. Ind. Eng. Chem.* 42 (2016) 36–45, <https://doi.org/10.1016/j.jiec.2016.07.025>.
- [35] J. Andraos, Global green chemistry metrics analysis algorithm and spreadsheets: evaluation of the material efficiency performances of synthesis plans for Oseltamivir Phosphate (Tamiflu) as a Test Case, *Org. Process. Res. Dev.* 13 (2008) 161–185, <https://doi.org/10.1021/op800157z>.
- [36] P. Tundo, P. Anastas, D.S.C. Black, J. Breen, T. Collins, S. Memoli, J. Miyamoto, M. Polyakoff, W. Tumas, Synthetic pathways and processes in green chemistry. introductory overview, *Pure Appl. Chem.* 72 (2000) 1207–1228, <https://doi.org/10.1351/pac200072071207>.
- [37] M.A. Tejero, E. Ramírez, C. Fité, J. Tejero, F. Cunill, Esterification of levulinic acid with butanol over ion exchange resins, *Appl. Catal. A-Gen.* 517 (2016) 56–66, <https://doi.org/10.1016/j.apcata.2016.02.032>.
- [38] G.E.P. Box, N.R. Draper, *Response Surfaces, Mixtures, and Ridge Analyses* 649, John Wiley & Sons, 2007.
- [39] J. Lima-Ramos, P. Tufvesson, J.M. Woodley, Application of environmental and economic metrics to guide the development of biocatalytic processes, *Green process. Synth.* 3 (2014) 195–213, <https://doi.org/10.1515/gps-2013-0094>.
- [40] J. Andraos, M. Sayed, On the use of “Green” metrics in the undergraduate organic chemistry lecture and lab to assess the mass efficiency of organic reactions, *J. Chem. Educ.* 84 (2007) 1004–1010, <https://doi.org/10.1021/ed084p1004>.
- [41] J. Andraos, Unification of reaction metrics for green chemistry: applications to reaction analysis, *Org. Process. Res. Dev.* 9 (2005) 149–163, <https://doi.org/10.1021/op049803n>.
- [42] J. Andraos, Unification of reaction metrics for green chemistry II: evaluation of named organic reactions and application to reaction discovery, *Org. Process. Res. Dev.* 9 (2005) 404–431, <https://doi.org/10.1021/op050014v>.
- [43] J. Andraos, A database tool for process chemists and chemical engineers to gauge the material and synthetic efficiencies of synthesis plans to industrially important targets, *Pure Appl. Chem.* 83 (2011) 1361–1378, <https://doi.org/10.1351/PAC-CON-10-10-07>.
- [44] R. Sheldon, The E Factor: fifteen years on, *Green Chem.* (2007) 1273–1283, <https://doi.org/10.1039/B713736M>.
- [45] D.J.C. Constable, A.D. Curzons, V.L. Cunningham, Metrics to “Green” Chemistry— which are the best? *Green Chem.* 4 (2002) 521–527, <https://doi.org/10.1039/b206169b>.
- [46] J.C. Gee, S. Fisher, Direct esterification of olefins: the challenge of mechanism determination in heterogeneous catalysis, *J. Catal.* 331 (2015) 13–24, <https://doi.org/10.1016/j.jcat.2015.08.010>.
- [47] O.S. Pavlov, S.A. Karsakov, S.Y. Pavlov, Processes of synthesis of 1-butene from 2-butene by the positional isomerization on sulfocation exchangers, *Russ. J. Appl. Chem.* 82 (2009) 1117–1122, <https://doi.org/10.1134/S1070427209060378>.
- [48] A. Moronta, J. Luengo, Y. Ramírez, J. Quiñónez, E. González, J. Sánchez, Isomerization of cis-2-butene and trans-2-butene catalyzed by acid- and ion-exchanged smectite-type clays, *Appl. Clay Sci.* 29 (2005) 117–123, <https://doi.org/10.1016/j.clay.2004.12.002>.
- [49] K. Jerábek, Characterization of swollen polymer gels using size exclusion chromatography, *Anal. Chem.* 57 (1985) 1598–1602, <https://doi.org/10.1021/ac00285a023>.
- [50] K. Jerábek, Determination of pore volume distribution from size exclusion chromatography data, *Anal. Chem.* 57 (1985) 1595–1597, <https://doi.org/10.1021/ac00285a022>.
- [51] B. Corain, M. Zecca, K. Jerábek, Catalysis and polymer networks — the role of morphology and molecular accessibility, *J. Mol. Catal. A Chem.* 177 (1) (2001) 3–20, [https://doi.org/10.1016/S1381-1169\(01\)00305-3](https://doi.org/10.1016/S1381-1169(01)00305-3).
- [52] K. Jerábek, L. Hanková, L. Holud, Working-state morphologies of ion exchange catalysts and their influence on reaction kinetics, *J. Mol. Catal. A Chem.* 333 (1–2) (2010) 109–113, <https://doi.org/10.1016/j.molcata.2010.10.004>.
- [53] J.H. Badia, C. Fité, R. Bringué, M. Iborra, F. Cunill, Catalytic activity and accessibility of acidic ion-exchange resins in liquid phase etherification reactions, *Top. Catal.* 58 (2015) 919–932, <https://doi.org/10.1007/s11244-015-0460-3>.
- [54] V. Russo, C. Rossano, E. Salucci, R. Tesser, T. Salmi, M. Di Serio, Intraparticle diffusion model to determine the intrinsic kinetics of ethyl levulinate synthesis promoted by Amberlyst-15, *Chem. Eng. Sci.* 228 (2020) 115974–115984, <https://doi.org/10.1016/j.ces.2020.115974>.
- [55] X. Tang, X. Zeng, Z. Li, W. Li, Y. Jiang, L. Hu, S. Liu, Y. Sun, L. Lin, In Situ generated catalyst system to convert biomass-derived levulinic acid to  $\gamma$ -Valerolactone, *ChemCatChem* 7 (2015) 1372–1379, <https://doi.org/10.1002/cctc.201500115>.
- [56] S.S. Enumula, V.R.B. Gurram, R.R. Chada, D.R. Burri, S.R.R. Kamaraju, Clean Synthesis of Alkyl Levulinates from Levulinic Acid over one Pot Synthesized WO<sub>3</sub>-SBA-16 Catalyst, *J. Mol. Catal. A-Chem.* 426 (2017) 30–38, <https://doi.org/10.1016/j.molcata.2016.10.032>.
- [57] S. Dutta, S. De, B. Saha, Alam Md. Advances in conversion of hemicellulosic biomass to furfural and upgrading to biofuels, *Catal. Sci. Technol.* 2 (2012) 2025–2036, <https://doi.org/10.1039/c2cy20235b>.